Published in final edited form as:
Science. 2011 July 22; 333(6041): 453–456. doi:10.1126/science.1207193.

De-AMPylation of the Small GTPase Rab1 by the Pathogen *Legionella pneumophila*

M. Ramona Neunuebel[1,*], **Yang Chen**[1,3,*], **Andrew H. Gaspar**[1], **Peter S. Backlund Jr**[2], **Alfred Yergey**[2], and **Matthias P. Machner**[1,†]

[1]Cell Biology and Metabolism Program, Eunice Kennedy Shriver National Institute of Child Health and Human Development, National Institutes of Health, Bethesda, MD 20892, USA

[2]Biomedical Mass Spectrometry Facility, Eunice Kennedy Shriver National Institute of Child Health and Human Development, National Institutes of Health, Bethesda, MD 20892, USA

[3]Health Science Center, Peking University, Beijing 100191, China

Abstract

The bacterial pathogen *Legionella pneumophila* exploits host cell vesicle transport by transiently manipulating the activity of the small guanosine triphosphatase (GTPase) Rab1. The effector protein SidM recruits Rab1 to the *Legionella*-containing vacuole (LCV), where it activates Rab1 and then AMPylates it by covalently adding adenosine monophosphate (AMP). *L. pneumophila* GTPase-activating protein LepB inactivates Rab1 before its removal from LCVs. Because LepB cannot bind AMPylated Rab1, the molecular events leading to Rab1 inactivation are unknown. We found that the effector protein SidD from *L. pneumophila* catalyzed AMP release from Rab1, generating de-AMPylated Rab1 accessible for inactivation by LepB. *L. pneumophila* mutants lacking SidD were defective for Rab1 removal from LCVs, identifying SidD as the missing link connecting the processes of early Rab1 accumulation and subsequent Rab1 removal during infection.

AMPylation (also known as adenylylation), the covalent attachment of adenosine monophosphate (AMP) to tyrosine or threonine side chains within target proteins, is used by bacterial pathogens to manipulate host cell signaling processes within infected cells (1–3). The intravacuolar pathogen *Legionella pneumophila* strain Philadelphia-1 exploits host cell endoplasmic reticulum to Golgi vesicle transport by modulating the activity of the small guanosine triphosphatase (GTPase) Rab1 (4). *L. pneumophila* delivers into the host cell the effector protein SidM (DrrA) that recruits Rab1 to the *Legionella*-containing vacuole (LCV) and activates it through guanosine diphosphate (GDP)/GTP exchange (5–8). Later during infection, the *L. pneumophila*GTPase-activating protein (GAP) LepB inactivates Rab1, thereby causing its release from the LCV membrane (8).

SidM AMPylates activated Rab1 by adding AMP to tyrosine-77, thereby disrupting Rab1 inactivation by GAPs such as LepB or mammalian TBC1D20 (3). Because Rab1 is transiently present on LCVs (8–10), we hypothesized that its removal from LCVs requires a

†To whom correspondence should be addressed. machnerm@mail.nih.gov.
*These authors contributed equally to this work.

Supporting Online Material
www.sciencemag.org/cgi/content/full/science.1207193/DC1
Materials and Methods
Figs. S1 to S17
Tables S1 and S2
References (*21–27*)

L. pneumophila protein that catalyzes de-AMPylation of Rab1, thereby rendering it accessible to GAPs. Indeed, we found that whole-cell lysate from *L. pneumophila* but not *Escherichia coli* efficiently removed radiolabeled [^{32}P]AMP from AMPylated Rab1 (see fig. S1 and supporting online materials and methods section).

Domains associated with AMPylation are evolutionarily conserved among prokaryotes and eukaryotes (11). However, the only protein de-AMPylase described to date is the bacterial glutamine synthetase adenylyl transferase (GS-ATase) (12), which precludes homology-based predictions to help identify the putative Rab1 de-AMPylase encoded by *L. pneumophila*. Genes of functionally linked proteins tend to be clustered within bacterial genomes and are often coinherited as modules (13). We noticed that the open reading frame adjacent to *sidM* encodes the translocated effector SidD (lpg2465) (14), a 507–amino acid protein of unknown function. *sidM* and *sidD* share conserved synteny across several *Legionella* isolates (fig. S2), indicating a potential functional relation. *sidD* deletion from *L. pneumophila* eliminated Rab1 de-AMPylase activity in bacterial lysate (Fig. 1A), allowing us to confidently attribute this activity to SidD.

Recombinant SidD efficiently removed radio-labeled [^{32}P]AMP from AMPylated Rab1 in a concentration-dependent manner, with an apparent specific activity of 6.5 μmol of product per minute times milligrams of enzyme (Fig. 1B). The decrease in radioactivity was not caused by proteolysis, because we found no evidence for Rab1 degradation by SidD (fig. S3). In fact, Rab1 repeatedly served as a substrate in multiple consecutive cycles of AMPylation and de-AMPylation catalyzed by sequential exposure to SidM and SidD, respectively (Fig. 1C). Rab35, which functions in endosomal trafficking, also served as a substrate in AMPylation and de-AMPylation reactions, whereas Rab2, Rab4, Rab6a, Rab8a, Rab14, and Rab15 showed no substantial AMPylation upon incubation with SidM, contrary to earlier reports (3).

We analyzed the products of the Rab1 de-AMPylation reaction. Mass spectrometric analyses of a tryptic digest of either unmodified, AMPylated, or de-AMPylated Rab1 showed a mass shift of the peptide $_{72}$TITSSYYR$_{79}$ (from 990 to 1319 daltons; here I, Ile; R, Arg; S, Ser; T, Thr; Y, Tyr) upon AMPylation (Fig. 2A), consistent with the addition of AMP (329 daltons) to tyrosine-77 within this peptide, as previously reported (3). Upon de-AMPylation by SidD, the AMPylated peptide returned to its original mass (990 daltons), indicating that AMP was removed from Rab1 to restore the original tyrosine-77 side chain (Fig. 2A and fig. S4). SidD also catalyzed removal of guanosine monophosphate (GMP) from GMPylated Rab1 (fig. S5), whereas cyclic AMP, a molecule with an internal phosphodiester bond, was not hydrolyzed by SidD (fig. S6), strongly suggesting that the mechanism of de-AMPylation/de-GMPylation differs from the mechanism for substrate recognition and/or hydrolysis by phosphodiesterases.

De-AMPylation catalyzed by GS-ATase generates ADP, not AMP, explaining why this process requires orthophosphate (15). In contrast, SidD catalyzed de-AMPylation of Rab1 in a phosphate-independent manner and generated AMP (Fig. 2, B and C), not ADP (fig. S7).

SidD's ability to target host Rab1 prompted us to look at the localization of exogenous SidD within mammalian cells. Rab1 primarily localizes to the Golgi compartment where it regulates docking and fusion of incoming transport vesicles (16). Green fluorescent protein (GFP)–tagged SidD produced in COS1 cells showed predominant perinuclear localization partially overlapping with that of giantin, a cis/medial Golgi marker, and TGN46, a trans-Golgi network marker (fig. S9). No colocalization of SidD with markers for other cellular organelle compartments was detected (fig. S10).

Disruption of Rab1 activity inhibits secretory vesicle trafficking, resulting in cell death (17, 18). AMPylation affects Rab1 binding to MICAL-3 and potentially other ligands (3), explaining why ectopic production of fluorescently labeled SidM causes Golgi fragmentation (6) and subsequent death in mammalian cells. Cytotoxicity detected in 92 ± 4% of cells producing mCherry-SidM was significantly reduced upon simultaneous production of GFP-SidD, but not GFP, with 45 ± 7% of doubly transfected cells showing normal nucleus morphology (Fig. 3, A and B). Similarly, whereas the majority (>99%) of COS1 cells displayed Golgi fragmentation upon production of even low levels of fluorescently (mCherry or GFP)–tagged SidM (Fig. 3, C and D) (6), 39 ± 2% of COS1 cells coproducing GFP-SidD and intermediate or low levels of mCherry-SidM showed limited or no Golgi fragmentation (Fig. 3, C and D) suggesting that SidD's de-AMPylase activity counteracted the inhibitory effect of AMPylation on Rab1 ligand binding, thereby attenuating Golgi fragmentation and subsequent cell death.

AMPylated GTP-Rab1 cannot be bound and inactivated by Rab1-GAPs such as $LepB_{1–1232}$ or $TBC1D20_{1–364}$ (variants lacking the predicted C-terminal transmembrane anchor), whereas unmodified Rab1 rapidly hydrolyses [γ^{32}P]GTP in their presence (fig. S11, A and B) (3). We hypothesized that SidD-mediated removal of AMP from tyrosine-77 in Rab1 would restore interaction of GTP-Rab1 with its specific GAPs, resulting in Rab1 inactivation through GTP hydrolysis. We found that in the presence of SidD inactivation of AMPylated Rab1 by $LepB_{1–1232}$ or $TBC1D20_{1–364}$ increased dramatically, confirming our hypothesis (Fig. 4, A and B).

LepB's GAP activity has been proposed to stimulate Rab1 inactivation and subsequent removal from LCVs, because an increase in LepB levels coincides with a decrease of Rab1 (and SidM) present on LCVs (8). We wanted to determine the role of SidD in the Rab1 removal process. In mouse bone marrow–derived macrophages, LCVs containing Δ*sidD* mutants displayed prolonged colocalization with host cell Rab1, with 38 ± 2% Rab1-positive LCVs four hours after uptake compared with only 6 ± 3% for wild-type (WT) *L. pneumophila* (Fig. 4, C and D). Thus, the de-AMPylation activity of SidD is critical for the ability of *L. pneumophila* to remove Rab1 from LCVs in a timely manner. A *L. pneumophila* Δ*lepB* mutant displayed a similar Rab1 removal defect to that of a Δ*sidD* mutant (Fig. 4D), supporting our hypothesis that both SidD and LepB are required for efficient Rab1 removal from LCVs. Unlike Δ*sidD* mutants, which were able to replicate at WT levels (fig. S12), Δ*lepB* mutants were attenuated for intracellular replication in human U937 macrophages (fig. S13), but not in liquid media (fig. S14). The replication defect of Δ*lepB* mutants was not likely to be a consequence of prolonged Rab1 colocalization with LCVs given that Δ*sidD* mutants, which display a similar Rab1 recruitment phenotype, replicated normally within host cells (fig. S12).

The antagonistic effects of SidD and SidMon Rab1 colocalization with LCVs (Fig. 4, C and D) led us to investigate the regulation of their translocation during infection. Using digitonin to selectively extract effector proteins from infected host cells (19), we found that SidD and LepB levels increased as SidM levels decreased, consistent with the idea that SidD and LepB are both required to remove Rab1 from LCVs after recruitment by SidM (Fig. 4, E and F and fig. S15). We observed a similar temporal regulation of effector protein production in liquid culture, where *L. pneumophila* mimics the biphasic life cycle found during infection (fig. S16) (20). Furthermore, premature translocation of SidD into host cells by Δ*sidD* mutants constitutively producing plasmid-encoded SidD strongly attenuated Rab1 accumulation on LCVs two hours after uptake compared with the WT strain (Fig. 3D), consistent with the idea that de-AMPylated Rab1 is rapidly inactivated and extracted from LCVs.

Our studies support a model in which *L. pneumophila* sequentially delivers its effector proteins into the host cytosol where they exploit Rab1 activity through a series of modification events (fig. S17). Early during infection, Rab1 is recruited to LCVs by the multifunctional effector protein SidM, which mediates release of Rab1 from its chaperone GDP dissociation inhibitor (RabGDI) (7, 8), Rab1 activation through GDP/GTP exchange, and AMPylation. AMPylated GTP-Rab1 is locked in the active conformation, which prevents its premature inactivation by host cell GAPs such as TBC1D20. AMPylated Rab1 could promote docking and fusion of secretory vesicles with LCVs until *L. pneumophila* translocates the de-AMPylase SidD into host cells. SidD catalyzes removal of AMP from GTP-Rab1, thereby enabling Rab1 inactivation by the GAP LepB and subsequent membrane extraction of GDP-Rab1 by RabGDI.

The identification of SidD as the Rab1 de-AMPylase not only provides the missing link in a complex chain of Rab1 modulation events during *L. pneumophila* infection, but also presents an intriguing example for how prokaryotic and eukaryotic cells could regulate protein function through transient AMPylation.

Supplementary Material

Refer to Web version on PubMed Central for supplementary material.

Acknowledgments

We thank G. Storz, S. Gottesman, J. Bonifacino, J. Neunuebel, and M. Barzik for critical reading and insightful discussion and R. Isberg and V. Losick for kindly providing reagents. This work was supported by the Intramural Research Program of the NIH.

References and Notes

1. Yarbrough ML, et al. Science. 2009; 323:269. 10.1126/science.1166382. [PubMed: 19039103]
2. Worby CA, et al. Mol. Cell. 2009; 34:93. [PubMed: 19362538]
3. Müller MP, et al. Science. 2010; 329:946. 10.1126/science.1192276. [PubMed: 20651120]
4. Ensminger AW, Isberg RR. Curr. Opin. Microbiol. 2009; 12:67. [PubMed: 19157961]
5. Murata T, et al. Nat. Cell Biol. 2006; 8:971. [PubMed: 16906144]
6. Machner MP, Isberg RR. Dev. Cell. 2006; 11:47. [PubMed: 16824952]
7. Machner MP, Isberg RR. Science. 2007; 318:974. 10.1126/science.1149121. [PubMed: 17947549]
8. Ingmundson A, Delprato A, Lambright DG, Roy CR. Nature. 2007; 450:365. [PubMed: 17952054]
9. Derré I, Isberg RR. Infect. Immun. 2004; 72:3048. [PubMed: 15102819]
10. Kagan JC, Stein MP, Pypaert M, Roy CR. J. Exp. Med. 2004; 199:1201. [PubMed: 15117975]
11. Roy CR, Mukherjee S. Sci. Signal. 2009; 2:pe14. [PubMed: 19293428]
12. Mantel M, Holzer H. Proc. Natl. Acad. Sci. U.S.A. 1970; 65:660. [PubMed: 4910853]
13. Spirin V, Mirny LA. Proc. Natl. Acad. Sci. U.S.A. 2003; 100:12123. [PubMed: 14517352]
14. Luo ZQ, Isberg RR. Proc. Natl. Acad. Sci. U.S.A. 2004; 101:841. [PubMed: 14715899]
15. Anderson WB, Stadtman ER. Biochem. Biophys. Res. Commun. 1970; 41:704. [PubMed: 4920873]
16. Plutner H, et al. J. Cell Biol. 1991; 115:31. [PubMed: 1918138]
17. Bacon RA, Salminen A, Ruohola H, Novick P, Ferro-Novick S. J. Cell Biol. 1989; 109:1015. [PubMed: 2504726]
18. Tisdale EJ, Bourne JR, Khosravi-Far R, Der CJ, Balch WE. J. Cell Biol. 1992; 119:749. [PubMed: 1429835]
19. Derré I, Isberg RR. Infect. Immun. 2005; 73:4370. [PubMed: 15972532]
20. Byrne B, Swanson MS. Infect. Immun. 1998; 66:3029. [PubMed: 9632562]

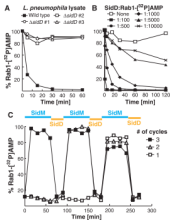

Fig. 1.

L. pneumophila SidD has Rab1 de-AMPylation activity. All de-AMPylation experiments were monitored by radioactive filter-binding assays measuring the levels of Rab1-[^{32}P]AMP, with each graph being a representative of at least three independent experiments. (**A**) *L. pneumophila* WT but not Δ*sidD* lysate has Rab1 de-AMPylation activity. Rab1-[^{32}P]AMP (1 μM) was incubated with lysate (100 μg) from *L. pneumophila* WT or three independently generated Δ*sidD* mutants (#1 to 3). (**B**) SidD is sufficient to de-AMPylate Rab1. Rab1-[^{32}P]AMP (1 μM) was incubated with purified glutathione *S*-transferase (GST)–SidD at the indicated molar ratios. (**C**) Rab1 can be repeatedly AMPylated and de-AMPylated. Three independent samples containing equal amounts of Rab1 (10 μM) were used in up to three consecutive cycles of AMPylation (blue) and de-AMPylation (orange) by incubation with SidM- and SidD-coated magnetic beads, respectively.

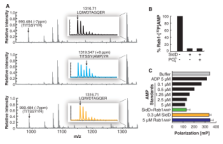

Fig. 2.

De-AMPylation catalyzed by SidD restores Rab1 and generates AMP. (**A**) Matrix-assisted laser desorption/ionization–time-of-flight reflector spectra of tryptic digestion of three samples. Mass errors of labeled peptides are shown in parts per million (ppm) relative to predicted values. (Top) Unmodified Rab1. (Middle) Rab1 with AMPylation showing loss of intensity of $_{72}$TITSSYYR$_{79}$ peptide, mass-to-charge ratio (*m/z*) 990, and existence of AMPylated peptide at *m/z* 1319. (Bottom) Rab1 after de-AMPylation. Peptide at *m/z* 1319 disappears and *m/z* 990 peptide reappears. The insets show magnification of the peaks around *m/z* 1319. A, Ala; D, Asp; E, Glu; G, Gly; L, Leu; Q, Gln; W, Trp. (**B**) Rab1 de-AMPylation by SidD is phosphate-independent. Rab1 (1 μM) was incubated in the presence (+) or absence (−) of GST-SidD or orthophosphate (as indicated). (**C**) SidD-catalyzed de-AMPylation of Rab1 generates AMP. AMP was detected by a competitive fluorescence polarization immunoassay. AMP and ADP standards are shown as positive and negative assay controls, respectively. Error bars indicate SD from three independent experiments.

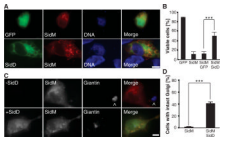

Fig. 3.

SidD protects cells from SidM-induced cytotoxicity and Golgi fragmentation. (**A**) SidD reduces SidM-induced cytotoxicity. COS1 cells cotransfected with plasmids encoding GFP (top panels) or GFP-SidD (bottom panels) and mCherry-SidM were fixed, and nuclei were labeled using Hoechst stain. (**B**) Quantification of (A) showing the percentage of cells with normal nuclear morphology. Data are mean ± SD (error bars) for three independent experiments. ***$P < 0.001$ (two-tailed *t* test). (**C**) COS1 cells producing mCherry-SidM only (−SidD; top panel) or mCherry-SidM and GFP-SidD (+SidD; bottom panel) were fixed and stained with the Golgi marker giantin. The merged images (right) show SidD (green), SidM (red), and giantin (blue). The ^ symbol denotes Golgi of a nontransfected cell. (**D**) Percentage of cells with intact Golgi structures are quantified. Data are mean ± SD from three independent experiments. ***$P < 0.001$ (two-tailed *t* test). (A and C) Scale bars, 1 μm.

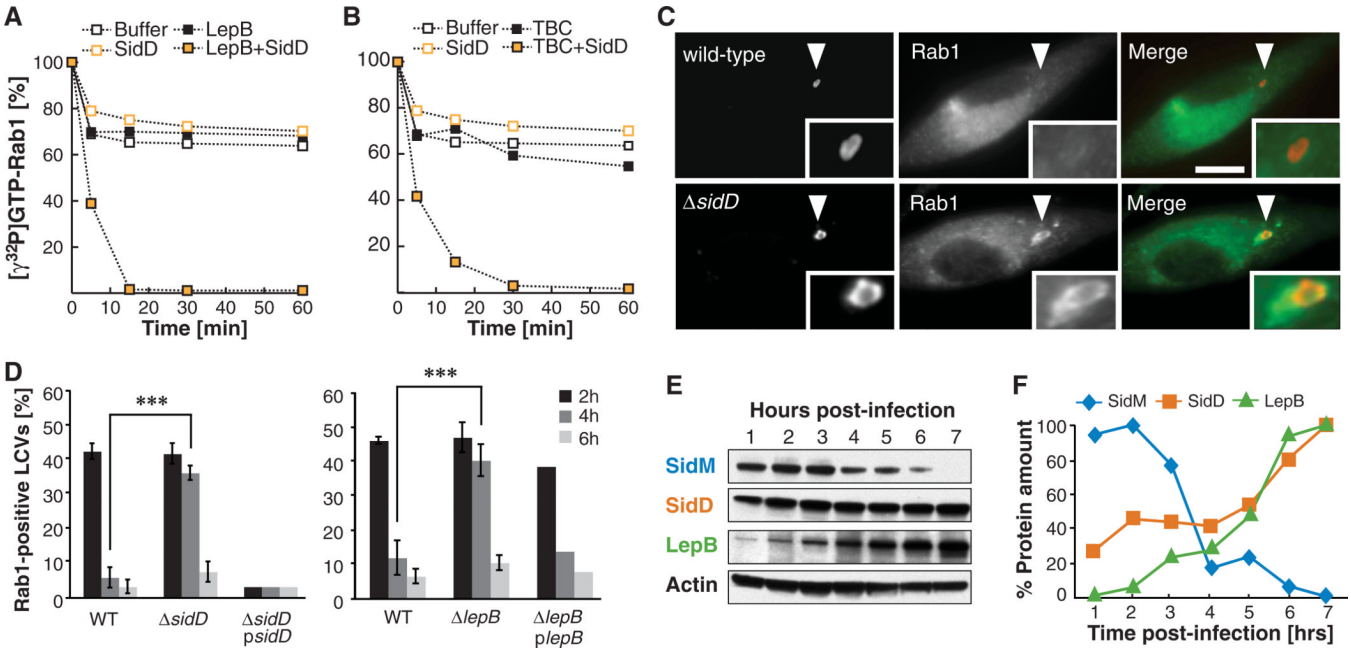

Fig. 4.

SidD is required for Rab1 inactivation by LepB and removal from LCVs. (**A** and **B**) De-AMPylation enables GAP-stimulated GTP hydrolysis by Rab1. GTP hydrolysis of Rab1-AMP (1 μM) loaded with [γ^{32}P]GTP in the absence or presence of GST-SidD (0.35 μM) and 40 nM His-LepB$_{1–1232}$ (A) or His-TBC1D20$_{1–364}$ (B). Rab1-[γ^{32}P]GTP levels were monitored over time by a filter-binding assay. Graphs are representatives of at least three independent experiments. (**C** and **D**) *L. pneumophila* Δ*sidD* mutants are defective for Rab1 removal from LCVs. Bone marrow–derived A/J mouse macrophages were challenged with the indicated *L. pneumophila* strains. (C) Examples of cells four hours after infection. Cells were fixed at the indicated time points and stained for intracellular bacteria (left panels;, WT or a Δ*sidD* mutant) and Rab1 (middle panels). Merged images (right panels) show bacteria in red and Rab1 in green. Arrowheads indicate locations of the LCVs magnified in the insets. Scale bar, 1 μm. (D) Percentile of LCVs showing colocalization with host cell Rab1 at the indicated times after infection. The graph shows means ± SD (error bars) from three independent experiments. ***$P < 0.001$ (two-tailed t test). (**E** and **F**) Temporal regulation of effector translocation. (E) U937 cells were challenged with *L. pneumophila* WT or a T4SS-defective mutant (Lp03) (fig. S14) and were lysed at the indicated time points using 1% digitonin. The digitonin-soluble fraction was analyzed by Western blot using antibody specific for the respective effector proteins. (F) Signals shown in (E) were quantified and normalized to the loading control (β-actin), with the maximum signal arbitrarily set to 100%. This graph is a representative of two independent experiments.